JOURNAL OF SOLID STATE CHEMISTRY 117, 309–317 (1995)

$[Cs^+(15\text{-Crown-5})(18\text{-Crown-6})e^-]_6 \cdot (18\text{-Crown-6})$: Properties of the First Mixed Crown Ether Electride

Michael J. Wagner[1] and James L. Dye[2]

Department of Chemistry and Center for Fundamental Materials Research, Michigan State University, East Lansing, Michigan 48824

Received August 25, 1994; in revised form November 25, 1994; accepted January 4, 1995

The sizes and structures of cavities and channels in the first crystalline mixed crown electride, $[Cs^+(18\text{-crown-6})(15\text{-crown-5})e^-]_6 \cdot (18C6)$, are reported and related to its properties. The structure consists of cesium cations complexed by one each of the 18-crown-6 and 15-crown-5 complexants, which pack to leave a remarkable ring of six cavities that are presumed to be the trapping sites of the excess electrons. The sizes and shapes of the cavities and connecting channels are described in detail with the aid of a newly developed computer program. The magnetic susceptibility (corrected for the low-temperature "tail" due to defect electrons) is shown to be consistent with that expected for an antiferromagnetically coupled 6-electron ring and yields an estimate of the coupling strength, J/k, of ~ -410 K. ^{133}Cs MAS NMR and the temperature dependence of the magnetic susceptibility show that the electron density at the cation nucleus is an order of magnitude smaller than that of either $Cs^+(18\text{-crown-6})_2e^-$ or $Cs^+(15\text{-crown-5})_2e^-$. The compound is moderately conductive with a lower limit of conductivity at 213 K estimated to be $2 \times 10^{-3}\ \Omega^{-1}\ cm^{-1}$. The dominant conduction mechanism is probably variable range hopping of defect electrons.

INTRODUCTION

Electrides are salts that contain complexed alkali metal cations, charge-balanced by stochiometrically trapped electrons. Electrides in which the cation is complexed by two crown ethers ("sandwiched") have been extensively studied (1–3). Specifically, $Cs^+(18\text{-crown-6})_2e^-$ (abbreviated $Cs^+(18C6)_2e^-$) and $Cs^+(15\text{-crown-5})_2e^-$ (abbreviated $Cs^+(15C5)_2e^-$), have been well characterized; the former by single crystal X-ray crystallography (4), NMR (5), EPR (6–8), powder conductivity (9–11), optical absorption spectroscopy (9, 12), DSC (5), and magnetic susceptibility (13–15), the latter by all the aforementioned techniques except EPR (16, 17). The possibility of the existence of an electride with cations sandwiched by two different crown ethers became apparent when $Cs^+(18C6)_2e^-$ was mixed with $Cs^+(15C5)_2e^-$ as a temperature reference during a ^{133}Cs NMR experiment; a third peak not due to either pure $Cs^+(18C6)_2e^-$ or $Cs^+(15C5)_2e^-$ appeared, which was attributed to a mixed-crown electride formed by a solid state reaction in the NMR rotor (17).

The structure and physical properties of the deliberately synthesized mixed crown electride are very different from those of either parent compound $[Cs^+(18C6)_2e^-$ or $Cs^+(15C5)_2e^-]$. The properties of this mixed-crown electride caused us to conclude that it is not a mixture of the two parent compounds but rather a new compound. Later, single crystal X-ray diffraction studies showed that this was indeed the case; each cesium cation is sandwiched between one 18-crown-6 *and* one 15-crown-5. Six such sandwiches are arranged around a central 18C6 molecule. In addition, the packing of the complexed cations leaves six-membered rings of cavities, which theory (18, 19) and experiment (8, 20) have indicated are the electron-trapping sites in electrides. The strong coupling among electrons in this case is rather surprising since the trapping sites in the parent electrides are rather isolated and show only weak magnetic coupling, although electron pairs do occur in K^+ (cryptand [2.2.2])e^- (21).The structure and properties of this fascinating new electride with six-membered electron rings, which has the empirical formula $[Cs(15C5)(18C6)]_6 \cdot 18C6$, have been described in a brief communication elsewhere (22); this paper describes the structure and properties in greater detail.

EXPERIMENTAL

$[Cs^+(18C6)(15C5)e^-]_6 \cdot (18C6)$ was synthesized by anaerobically dissolving cesium and approximately 10% excess of a 1:1 mixture of 18-crown-6 and 15-crown-5 in dimethyl ether in a modified H-cell (23). The reaction vessel was cooled in dry ice during evacuation to prevent the loss of the more volatile 15-crown-5. Care was taken to ensure that the reaction mixture never exceeded 220 K in order to prevent thermal decomposition. Crystals were formed by addition of trimethylamine, further cooling to dry ice temperature and slowly reducing the volume

[1] Present address: Department of Chemistry, Massachusetts Institute of Technology, Cambridge, MA 02139.

[2] To whom correspondence should be addressed.

0022-4596/95 $12.00

of primary solvent (~1–2 weeks). Crystals were dried under vacuum, collected under an inert atmosphere, and stored in liquid N_2. Due to the extreme sensitivity of this electride to thermal and oxidative decomposition, sample manipulation was always performed under an inert atmosphere on aluminum supports immersed in liquid N_2. Details of the purification of materials and of the synthetic methods used have been described elsewhere (24).

The ^{133}Cs spectra were measured at the Max T. Rogers NMR facility at Michigan State University on a 9.3950 Tesla Varian VXR 400S NMR spectrometer utilizing a Doty dual bearing VT-MAS probe. Samples were spun at 4 KHz, a 2.4-msec pulse length was employed with 5- to 15-sec postacquisition delay times and the signal was averaged over 64 transients. The rotors were loaded into the precooled probe in a nitrogen-filled glove bag. A dewar of liquid nitrogen was utilized not only to store the sample but also to limit the humidity in the bag. Sample temperature was calibrated with a thermocouple attached to the brass rotor guide pin while spinning an empty rotor at the same speed and gas pressures as had been used in obtaining the spectra.

Magnetic susceptibility measurements were made with an S.H.E. 800 Series SQUID susceptometer. Samples were run in Kel-F buckets and transferred to the SQUID in a nitrogen-filled glove bag. A large copper block was cooled to liquid-nitrogen temperature and inserted into the loading mechanism immediately prior to loading the liquid-nitrogen-cooled sample. The block acted as a heat sink to ensure that the sample's temperature did not rise much above liquid N_2 temperature during evacuation and backfilling of the antechamber. The electronic contribution to the susceptibility was calculated by subtracting the diamagnetic contribution of the decomposed sample and the bucket.

Pressed powder and pellet dc conductivity measurements were made as a function of temperature and voltage with a Keithley 617 programmable electrometer. Impedance spectroscopy measurements were made with a Hewlett-Packard 4192A-LF impedance analyzer over the frequency range of 5 Hz to 13 MHz. Application of potassium metal to the electrodes was accomplished in a helium-filled glove box; the sample and conductivity cell were kept below 200 K in a cold well during the loading. Samples for measurements that did not require alkali metal electrodes were loaded in a nitrogen-filled glove bag. Further details of the methods employed are published elsewhere (10, 11).

RESULTS AND DISCUSSION

The crystal structure has been described elsewhere (22) but only a schematic description of the cavities and connecting channels was given. The compound crystallizes in the $R\bar{3}$ space group. Each cesium cation is complexed by an 18C6 and a 15C5 molecule. These sandwiched cations pack alternately above and below the plane of a central "free" (i.e., noncomplexing) 18C6 molecule. A threefold symmetry axis runs through the middle and perpendicular to the plane of the free crown. The sandwiched cations form a double three-bladed propeller about this axis; they are tilted 60° with respect to the plane of the free crown, with the upper three tilted in the opposite sense of the lower three. The structure is shown in color from two perspectives in Fig. 1 of Ref. (22).

The packing of the molecules leaves cavities arranged around and alternately above and below the plane of the free crown ether. At the time of the preliminary publication of this work (22) the nature of the cavities and channels could only be deduced by examining cross-sectional "slices" of the structure. As a result, only a schematic description could be given (Fig. 2 of Ref. (22)). Since then, we have developed a method that permits accurate determination of the sizes of the channels and cavities and a display of their shapes and connectivities. A detailed description of the methodology will be published elsewhere (25).

The positions of all atoms in a crystal structure and their van der Waals radii are used to produce a 40 × 40 × 40 grid of points with each point assigned a value that corresponds to its distance from the nearest van der Waals surface. (Internal points are assigned a value of zero.) By using the commercial program AVS (26) on a Silicon Graphics computer, "isosurfaces" are produced from the smoothed grid point values such that all points on a given surface are at the same distance from the surfaces of the atoms. By observing the distance at which a given channel just breaks, one can determine the minimum diameter of the channel. Similarly, by noting the distance at which a cavity just disappears, the *minimum* diameter of a sphere that would just fit into the cavity can be determined. While the true shapes of the cavities and channels could, in principle, be determined by setting the distance to the smallest nonzero values, in practice this is not useful since all cracks and crevices then appear and the filled foreground tends to hide the channels and cavities. Thus, a compromise is reached that shows the correct locations and connectivities of the cavities and channels, but at a size that is reduced in all directions from the true size by a known amount.

Figure 1 shows a view down the threefold (c) axis of an isosurface of the mixed sandwich electride. Each point on this surface is 0.55(2) Å from the nearest atomic van der Waals surface. (The number in parentheses represents the uncertainty in the last digit that results from the finite grid size and the smoothing procedure.) The largest cavities (E) have a complex shape and could accommodate a hard sphere of diameter 3.69(3) Å. These cavities form a

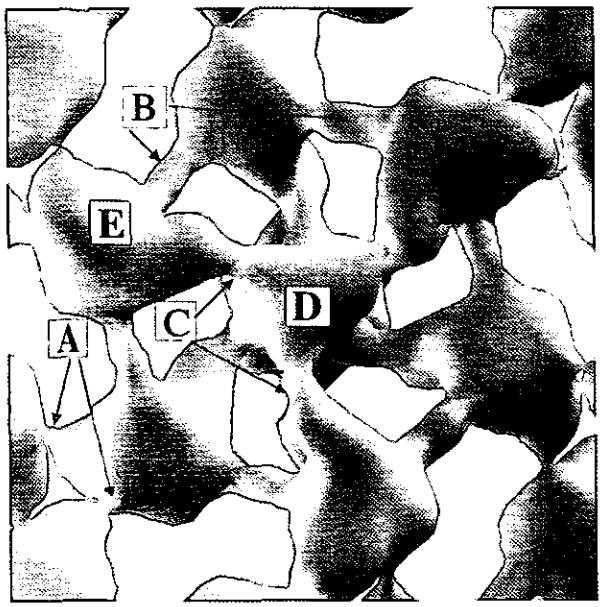

FIG. 1. View of the cavities and channels down the threefold (c) axis. Each point on this isosurface and on those shown in Fig. 2 is 0.55 ± 0.02 Å from the nearest van der Waals surface of the atoms in the structure. See text for channel and cavity sizes.

six-membered ring about the free crown with short (~8 Å center-to-center), channels (B) of minimum diameter 1.18(3) Å that connect each cavity with its two nearest neighbors in the ring. These major cavities (E) are located alternately above and below the plane of the central crown ether. Each cavity is also connected to two neighboring six-membered rings by longer (~10 Å center-to-center) more constricted channels (A) of minimum diameter 1.10(3) Å to complete a three-dimensional network of cavities and channels. Additionally, there are two smaller and more spherical cavities (D) located above and below the plane of the free crown ether that serve as cationic sites for the approximately 4.5 mole% excess cesium as observed in the crystal structure (22).This dopant level corresponds to one in four free crown ethers being coordinated to a Cs^+ ion. The diameter of a hard sphere that could just fit into one of these cavities is 2.91(6) Å, which is compatible with the ionic diameter of Cs^+ (3.38 Å), considering the "soft" nature of van der Waals surfaces. Bent channels (C) of minimum diameter 1.22(6) Å connect these central cavities with each of the ring cavities. The cavity shapes are shown in greater detail and from various directions in the isosurfaces displayed in Fig. 2. A side view of the two cavities (D) above and below the central crown ether is shown in Fig. 2a. Channel (F) has a minimum diameter of 2.40(2) Å and corresponds to the hole through the center of the 18-crown-6 molecule. Note that a K^+ ion of diameter 2.66 Å is commonly found in the center of an 18-crown-6 molecule. The difference between the size of a K^+ ion and the hole size found by the present method results from the hard sphere nature of the model used here. This problem is similar to that encountered when using solid space-filling models of molecules and is not unexpected, since van der Waals surfaces are somewhat soft and can deform to accommodate larger ions than the hard sphere model would indicate.

A close-up view of the major cavity (E) and the channels (A), (B), and (C) is shown in Fig. 2b. This is a view of one of the "bottom" cavities of Fig. 1 from the same direction. Figure 2c shows a side view of the same cavity that emphasizes the elongation of the cavity (E) along a roughly vertical direction. Also shown in Fig. 2c is a small channel (G), of minimum diameter 1.00(2) Å, that connects each major cavity (E) with a new cavity (H) that is centered on the threefold axis and could accommodate a sphere of diameter 2.91(6) Å, the same as cavity (D). The cavity–channel structure of this electride is so complex that it is virtually impossible to describe it without the pictures that are made possible with the new display program (25).

The electronic contribution to the molar magnetic susceptibility of two samples of $[Cs^+(15C5)(18C6)e^-]_6 \cdot 18C6$ is shown in Fig. 3. The differences seen at low temperature are probably due to differences in the amount of excess cesium included during synthesis. The susceptibilities of both samples are independent of the field between 0.5 and 7 kG. The data display no maximum and, rather than tending toward Curie–Weiss law behavior, the susceptibility rises with increasing temperature after reaching a minimum caused by the paramagnetic "tail." The high-temperature susceptibility corresponds to less than 13 and 3% of the total number of electrons expected from the stoichiometry at 200 and 80 K, respectively. Allowing the temperature to rise above about 230 K results in an apparently irreversible change to more Curie-like behavior. Multiple warmings resulted in a much stronger signal, perhaps through thermally created defect sites or an order–disorder transition. The magnetic behavior of this mixed sandwich electride is in sharp contrast to those of the two parent compounds which are antiferromagnets with maxima in their susceptibilities and a nearly stoichiometric number of independent spins at high temperatures (14, 17)

As shown by Figs. 1 and 2, the cavity–channel structure of this electride is very complex. We anticipate that the electrons released by ionization of Cs to yield complexed Cs^+ and trapped electrons would have their maximum density in the largest cavities (E). If so, the strongest interelectron coupling would be through the shortest open channels (B), which connect six cavities to form a puckered ring. Weaker, but still substantial, coupling to other rings through channels of type (A) would also be expected. The crystal structure shows that excess Cs^+ ions occupy

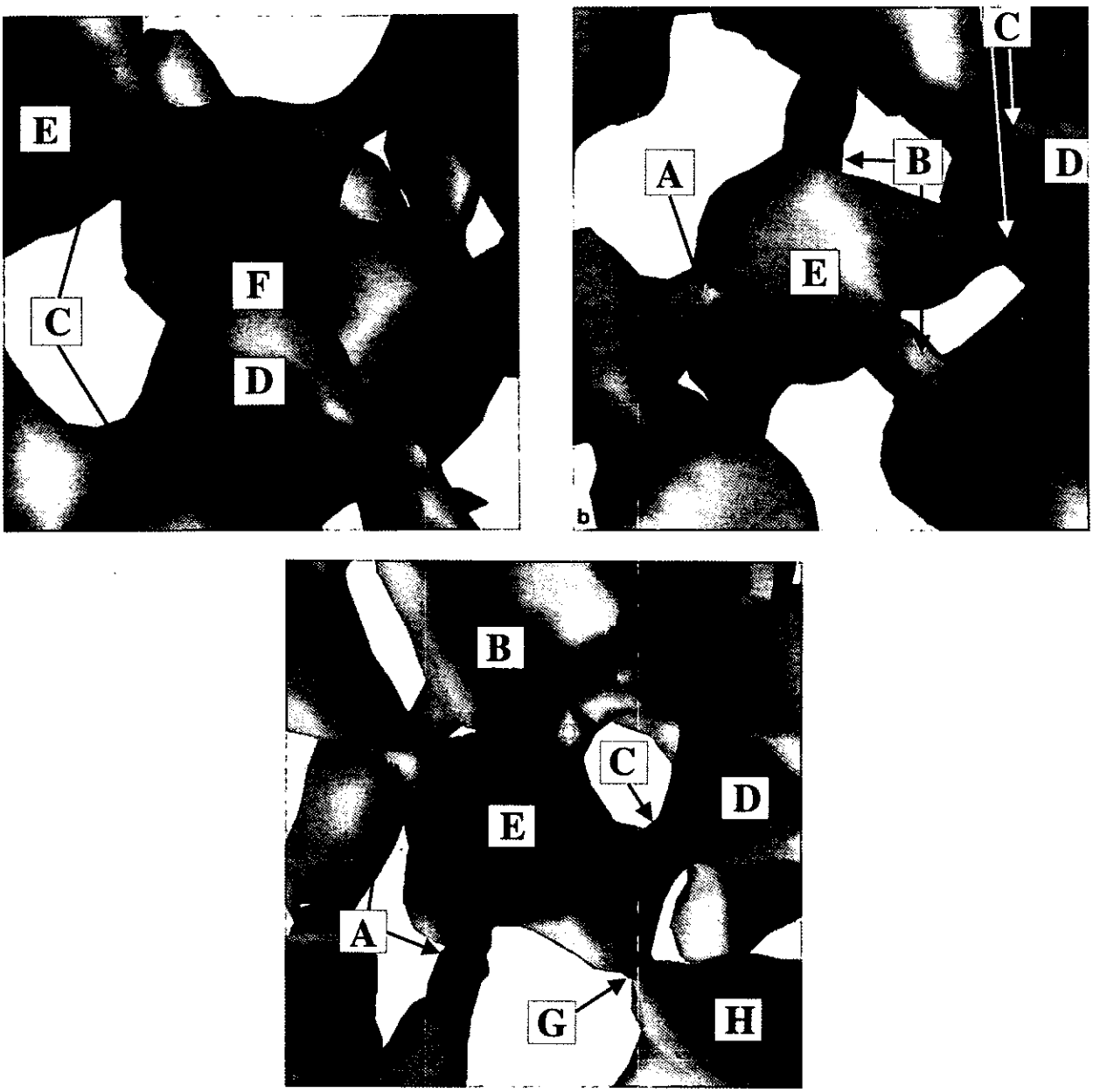

FIG. 2. Close-up views of the cavities and channels. The labels are consistent with those in Fig. 1. (a) View perpendicular to the *c* axis that shows the pair of cavities (D) above and below the central 18-crown-6 molecule. The "pinched" region (F) represents the hole through this crown ether. The connecting channels (C) to the major cavities (E) are also apparent in this figure. (b) View of a major cavity (E) along a direction parallel to the *c* axis and of the channels that connect it to other cavities. (c) Side view of the major cavity (E) that shows its elongation and connection to a cavity (H) that is centered on the *c* axis midway between two cavities of type (D). Channel (G) has a minimum diameter of 1.00 ± 0.02 Å.

positions (D) above or below the central crown ether. A likely trap for the defect electron released by ionization of Cs is cavity (H). This is close enough to the excess Cs^+ ion to yield reasonable charge balance, but far enough from the central crown ether to avoid the repulsive effects of the crown ether oxygens. As described below, the low temperature susceptibility tail reflects the presence of these defect electrons, while the high-temperature behavior results from the stoichiometric trapped electrons that occupy cavities of type (E).

The structure of the mixed crown electride thus suggests that the dominant coupling between the trapped electrons is within the six-membered rings. The inter-ring connections are longer and more constricted, although

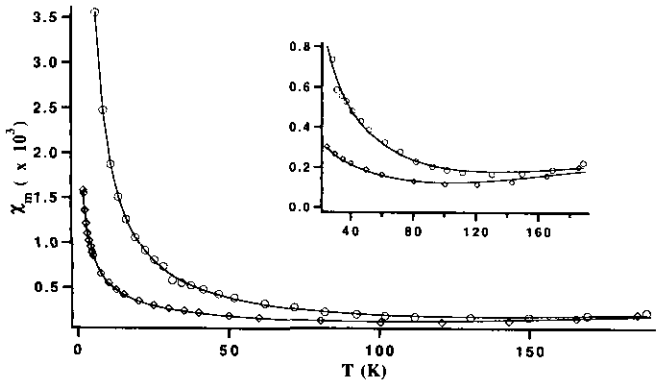

FIG. 3. The temperature dependence of the electronic molar susceptibility for two separate syntheses with different concentrations of "excess" cesium. The solid lines are nonlinear least-squares fits by an independent six-electron ring model together with a Curie-type "tail" (Eq. [4]). The inset is an expansion of the high-temperature region.

they may provide important 3D connections. Within the rings, the nearest neighbors are connected by rather open channels that should afford strong, nonorthogonal overlap. Neglecting inter-ring and second nearest neighbor intra-ring interactions, the Hamiltonian representing the exchange interaction of a six-membered Heisenberg ring is given by

$$\mathcal{H} = -2J\left(\sum_{i=1}^{5} \hat{S}_i \cdot \hat{S}_{i+1} + \hat{S}_6 \cdot \hat{S}_1\right) - g\beta \sum_{1}^{6} H \cdot \hat{S}_i \quad [1]$$

The energy levels for $S = 1/2$ six-membered rings governed by this Hamiltonian have been published (27) and yield a temperature dependence of the zero field susceptibility that is given by

$$\chi_m = \frac{Ng^2\beta^2}{6kT}\left\{\frac{\begin{array}{l}28 + 20\exp(x) + 4\exp(1.4385x) + 2\exp(2x) \\ + 2\exp(2.7639x) + 20\exp(3x) + 10\exp(4x) \\ + 4\exp(5x) + 4\exp(5.5616x) + 2\exp(7.2361x)\end{array}}{\begin{array}{l}7 + 10\exp(x) + \exp(1.3945x) + 6\exp(1.4385x) \\ + 3\exp(2x) + 3\exp(2.7639x) + 10\exp(3x) \\ + 7\exp(4x) + 6\exp(5x) + 6\exp(5.5616x) \\ + \exp(6x) + 3\exp(7.2361x) + \exp(8.6056x)\end{array}}\right\}, \quad [2]$$

where $x = -J/kT$. In addition to the magnetic moment due to the six-electron rings, allowance must be made for contributions to the susceptibility from paramagnetic trapped electrons from the excess cesium and for uncorrected diamagnetism and temperature independent paramagnetism (TIP). The trapped electrons are assumed to follow a Curie-like law

$$\chi_{para} = \frac{C}{T^n}. \quad [3]$$

The total susceptibility of this model can then be represented by the sum of the three terms

$$\chi = \chi_m + \chi_{para} + \chi_{dia}, \quad [4]$$

where χ_{dia} is a small, temperature-independent term used to account for any uncorrected diamagnetism and TIP. Nonlinear least-squares fitting of the data by Eq. [4] resulted in excellent fits for the two separately synthesized samples as shown in Fig. 3. In each case, the spectroscopic g value was held at that of the free electron. The fitting parameters for the sample with the more paramagnetic tail are $C = 0.02123(5)$, $n = 1.01(1)$, $J/k = -420(20)$, and $\chi_{dia} = -2(2) \times 10^{-5}$. The value of n for this sample indicates that the defect electrons obey the Curie law (are uncorrelated) and the value of C indicates that the tail can be accounted for by approximately 5.6 mole% unpaired spins. The fitting parameters for the sample with the smaller tail (Fig. 3) are $C = 0.00240(1)$, $n = 0.62(1)$, $J/k = -410(10)$, and $\chi_{dia} = -3(1) \times 10^{-5}$. The fits of the data, while over an admittedly limited temperature range due to the thermal instability and large coupling parameter of this electride, are at least consistent with the independent six-membered electron ring model that the structure suggests. It should be noted that the increase in susceptibility with temperature is much too gradual to be accounted for by simple spin-pairing.

The size of the Curie tail is preparation-dependent, as one would expect for defect electrons. In most samples, the low temperature data could be fit well by the Curie law plus a temperature-independent diamagnetic correction and the value of the Curie constant corresponded to up to 4–5% excess electrons. This number is in good agreement with the observed excess Cs^+ level seen in the X-ray structure and is therefore likely to be due to the electron released by the excess cesium. The sub-Curie law value of the exponent in the case of the sample with a much smaller tail than the others (Fig. 3) is characteristic of linear chain systems (28). This behavior has been explained in two different ways: the REHAC model (29) and the segment model (30). The former model explains the phenomenon by invoking a random distribution of exchange values which effectively divides the chain into weakly interacting segments, resulting in a low-temperature increase in χ which is weaker than T^{-1}. The latter explanation proposes that the behavior is the result of interspersed paramagnetic odd and diamagnetic even length chains. It seems likely that the electrons released by the excess Cs^+ tend to localize in the cavities (H) left open between adjacent free crown ether molecules along the c axis. Overlap with electrons in the rings via channels of type (H) might then lead to the chain-like behavior seen in the low-temperature susceptibility. However, it is unclear to us why this chain-like sub-Curie behavior

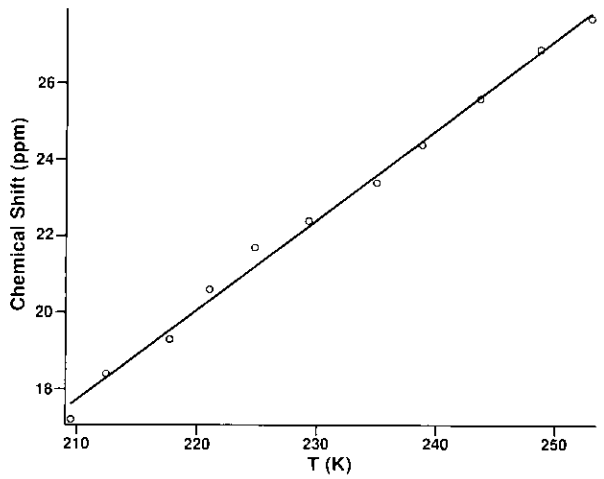

FIG. 4. ^{133}Cs NMR chemical shift plotted as a function of temperature. The solid line is a least-squares fit by Eq. [6].

does not also occur at higher dopant levels. It is, of course, possible that the sample that shows sub-Curie law behavior had a *deficiency* of cesium, leaving some rings with only five trapped electrons.

The ^{133}Cs NMR chemical shift of $[Cs^+(15C5)(18C6)e^-]_6 \cdot 18C6$ is very different from that of either of the other two electrides; it is by far the smallest of the three, more than 115 and 530 ppm smaller than those of $Cs^+(18C6)_2e^-$ and $Cs^+(15C5)_2e^-$, respectively, at 210 K (5, 17). The chemical shift of the mixed crown electride shifts paramagnetically with increasing temperature (Fig. 4), the *opposite* trend to that observed for either of the parent compounds. The shift depends linearly on temperature with a slope of 0.235(6) ppm K^{-1} and an intercept of $-32(1)$ ppm. Allowing the temperature to rise above ~250 K resulted in a slow, but significant and irreversible paramagnetic change of the chemical shift.

$[Cs^+(15C5)(18C6)e^-]_6 \cdot 18C6$, like $Cs^+(18C6)_2e^-$ and $Cs^+(15C5)_2e^-$, exhibits a ^{133}Cs contact (Knight) shift due to interaction with the electride electrons (5, 17). The unpaired electron contact density at the cation nucleus ($\langle|\psi(0)|^2\rangle$) is related to the Knight shift [$K(T)$] by

$$K(T) = \left(\frac{8\pi}{3N_{av}}\right)\langle|\psi(0)|^2\rangle\chi(T), \qquad [5]$$

where $\chi(T)$ is the electronic contribution to the magnetic susceptibility, and all other symbols have their usual meanings (31). $K(T)$ is approximately proportional to T since, in the limited temperature range studied by NMR, $\chi(T)$ is approximately proportional to T. $K(T)$ can therefore be closely approximated (in ppm) by

$$K(T) = \sigma(T) - \sigma(\infty) = 0.235\,T. \qquad [6]$$

The electronic part of the molar susceptibility at 210 K is 2.80×10^{-3} emu/mole. By using these data and the method more fully described elsewhere, (5) the atomic character can be calculated at 210 K to be $4.8(1) \times 10^{-3}\%$. This value is an order of magnitude smaller than that calculated for $Cs^+(18C6)_2e^-$ and $Cs^+(15C5)_2e^-$ (5, 17). It must be noted that thermal expansion of the compound may cause longer average Cs–O distances as the temperature is raised, resulting in a diamagnetic change in the Ramsey (32) shift, which would also be linear in temperature. This would in effect counteract the paramagnetic Knight shift with increasing temperature resulting in an erroneously small calculated atomic character. However, the temperature dependence due to the change in the Ramsey shift is expected to be small; a temperature-independent chemical shift is seen in all $Cs(18C6)_2$ and $Cs(15C5)_2$ salts and alkalides except $Cs^+(18C6)_2Cs^-$, an exception due to the effect of the structural perturbation caused by the large size of the cesium anion (5). Thus, the calculated atomic character of the trapped electron should be a good approximation, although it is a lower limit. Its exceedingly small value demonstrates an extraordinary exclusion of the electride electron from the Cs nucleus and is testament to the tighter complexation or "fit" provided by the mixed crown system vs the single crown systems.

As with the other physical properties, the electrical conductivity of $[Cs^+(15C5)(18C6)e^-]_6 \cdot 18C6$ is very different from those of the parent electrides, which exhibit very low electronic conductivities ($\sim 10^{-10}\ \Omega^{-1}\ cm^{-1}$ at 200 K) (11). Packed powder dc conductivity data were collected from 81 K to room temperature (Fig. 5). The apparent activation energies (E_a) can be calculated from the familiar Arrehenius relation

$$\sigma = \sigma_0 \exp(-E_a/kT), \qquad [7]$$

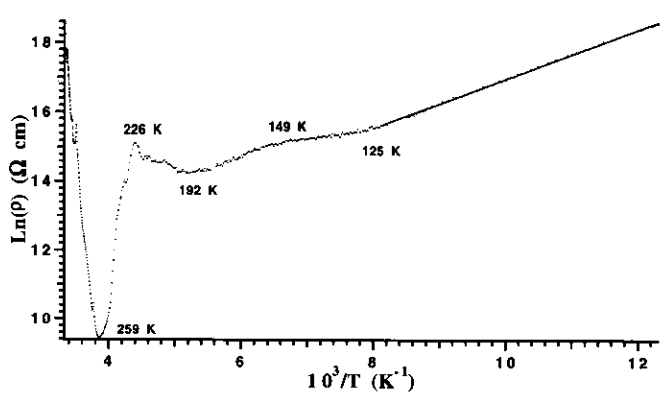

FIG. 5. The natural log of the packed powder dc resistance plotted against inverse temperature. The superimposed line in the low-temperature region is a fit by Eq. [7].

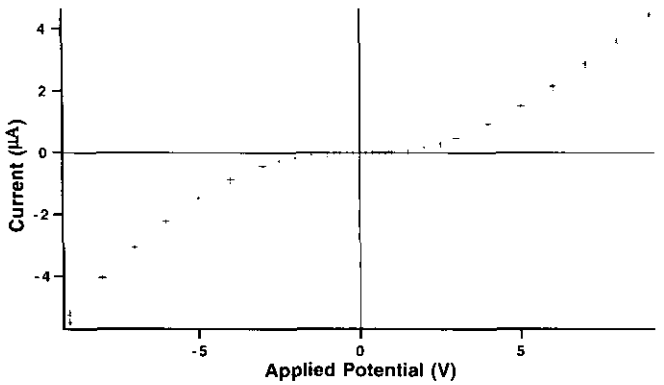

FIG. 6. Current–potential (I–V) curve for the packed powder at 162 K showing pronounced non-Ohmic behavior.

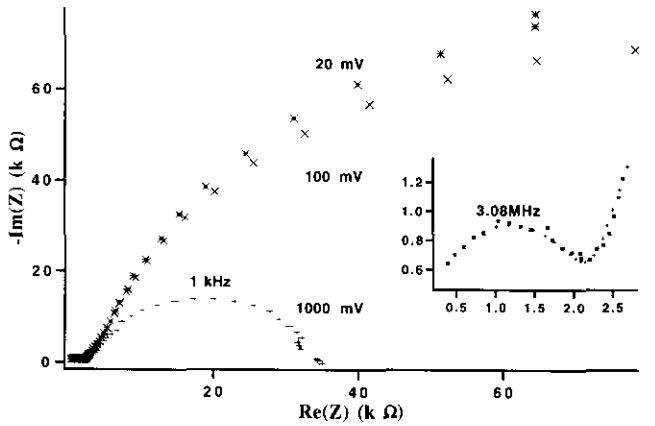

FIG. 7. Impedance spectroscopy arcs of packed powders between two bare steel electrodes at 160 K. The applied voltages and the frequencies of the arc maxima are indicated in the figure. The inset is an expansion of the high-frequency arc.

where σ is the measured conductivity. A fit to the low-temperature (81–125 K) behavior yields an apparent activation energy of 0.06 eV. The data between 125 and 192 K show two other linear regions with somewhat smaller apparent activation energies. Above 192 K the resistivity rises, reaching a maximum value at 226 K followed by a sharp decrease to 259 K where the resistivity again rises; the final rise is presumably due to decomposition. The initial rise is unlikely to be due to a semiconductor–metal transition since such a transition is not indicated by any other measurement including impedance spectroscopy described below. The rise and fall in resistivity could be due to electrode contact effects and is similar to that seen in $Cs^+(18C6)_2e^-$ (11).

The dc conductivity is markedly non-Ohmic, as seen in Fig. 6. This fact and the rather large resistance seen in the 2-probe DC conductivity measurements indicate the possibility of a Schottky barrier or oxide layer at the contacts. Complex ac 2-probe impedance measurements (Fig. 7) with bare steel electrodes show at least two resolvable arcs. The higher impedance (lower frequency) arc is strongly bias dependent also indicating an electrode effect. The electrodes were coated with potassium metal and the impedance spectroscopy measurements were repeated on pressed pellets. This resulted in a much lower resistance and a smaller dependence on the applied bias voltage (Fig. 8). This indicates that the outer arc and much of the resistance seen is due to a Schottky barrier, since the work function of potassium is expected to more closely match that of the electride. In addition, measurements with potassium-coated electrodes indicate only one arc with a zero frequency resistance at least an order of magnitude smaller than the smaller of the two seen with bare steel electrodes. Instrumental limitations prevented us from checking for the existence of higher frequency arcs. The measured arc may be from intergrain transport and contact resistances, in which case the intrinsic resistance of the sample would be lower than our measurements show. The temperature dependence of the zero frequency resistance, measured with potassium coated electrodes, was shown in Fig. 3 of the earlier communication (22). It should be noted that allowing the temperature to rise above 230 K resulted in an irreversible increase in the resistance. The temperature dependence of the zero frequency intercepts from the impedance spectroscopy data could be approximately fit with a single exponential with an apparent activation barrier of 0.064(2) eV. The fit of the data by this model of simple activated charge transport across a well-defined bandgap appeared to be reasonable at first glance, but examination of the residuals clearly showed the presence of reproducible systematic deviations. A much better fit without systematic deviations was obtained (22) by the equation

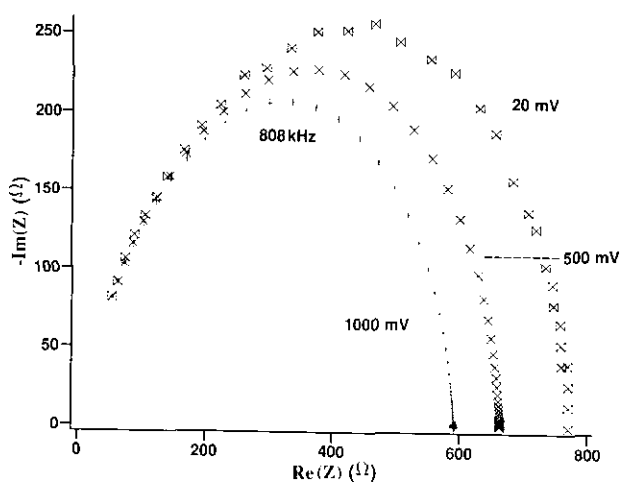

FIG. 8. Impedance spectroscopy arcs of a pressed pellet between two potassium-coated electrodes at 137 K.

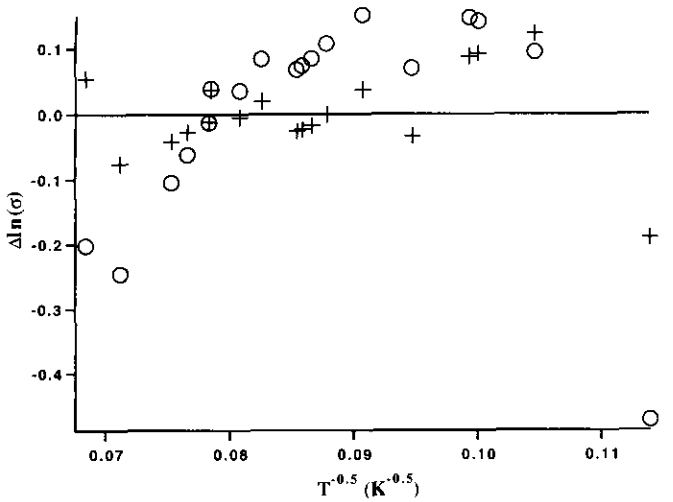

FIG. 9. Deviation of $\ln(\sigma)$ from inverse T behavior (circles, Eq. [7]) and from inverse $T^{1/2}$ behavior (crosses, Eq. [8]).

$$\sigma = \sigma_0 \exp[-(T_0/T)^{0.5}] \qquad [8]$$

with $\sigma_0 = 22.2(7)\ \Omega^{-1}\ \text{cm}^{-1}$, $T_0 = 1.80(2) \times 10^4$ K (see Fig. 9). This behavior is indicative of one of three general transport mechanisms: granular metallic (33–35), variable-range hopping in the presence of a Coulomb gap (36) and quasi-one-dimensional variable-range hopping (37).

The granular metallic mechanisms require a nonvanishing density of states at the Fermi level. Our susceptibility data indicate that there is a gap at the Fermi level and thus the granular metallic models are inappropriate. Therefore the conductivity is most likely to be due to a variable-range hopping mechanism, where the parameter T_0 depends inversely on the carrier localization length. The conductivity may be due to hopping of defect electrons or holes rather than intrinsic conductivity. The conductivity of other electrides has been shown to be largely due to defects (10, 11, 38); large Coulombic repulsions are expected to inhibit the mobility of the intrinsic electride electrons (18).

CONCLUSIONS

$[Cs^+(15C5)(18C6)e^-]_6 \cdot 18C6$ demonstrates the diversity of structural possibilities that can be found in electrides. The simple combination of crown ethers which results in this electride and its remarkable six-electron ring is testament to further diversity one might find with other, as yet undiscovered, electrides. The dramatic differences in the properties of this electride and its two parent compounds indicates the wide variation of properties that can occur with seemingly minor alterations of the complexants used. Further exploration of this young field through the use of other complexants and combinations of complexants might well yield other structures with novel optical, magnetic, and electronic properties.

ACKNOWLEDGMENTS

We are grateful to Tibor F. Nagy and Gregor Overney for developing the programs used to display cavity-channel isosurfaces. This research was supported by NSF Solid State Chemistry Grants DMR 90-17292 and DMR 94-02016 and by the Michigan State University Center for Fundamental Materials Research.

REFERENCES

1. M. J. Wagner and J. L. Dye, *in* "Molecular Recognition: Receptors for Cationic Guests" (G. W. Gokel, Ed.), Vol. 1. Pergamon, Oxford, UK in press.
2. M. J. Wagner and J. L. Dye, *Annu. Rev. Mater. Sci.* **23,** 223 (1993).
3. J. L. Dye, *Chemtracts: Inorg. Chem.* **5,** 243 (1993).
4. S. B. Dawes, D. L. Ward, R. H. Huang, and J. L. Dye, *J. Am. Chem. Soc.* **108,** 3534 (1986).
5. S. B. Dawes, A. S. Ellaboudy, and J. L. Dye, *J. Am. Chem. Soc.* **109,** 3508 (1987).
6. A. Ellaboudy, Ph.D. Dissertation, Michigan State University, East Lansing, 1984.
7. D. H. Shin, Ph.D. Dissertation, Michigan State University, East Lansing, 1992.
8. D. H. Shin, J. L. Dye, D. E. Budil, K. A. Earle, and J. H. Freed, *J. Phys. Chem.* **97,** 1213 (1993).
9. A. Ellaboudy, J. L. Dye, and P. B. Smith, *J. Am. Chem. Soc.* **105,** 6490 (1983).
10. K. J. Moeggenborg, Ph.D. Dissertation, Michigan State University, East Lansing, 1990.
11. K. J. Moeggenborg, J. Papaioannou, and J. L. Dye, *Chem. Mater.* **3,** 514 (1991).
12. A. Ellaboudy, M. L. Tinkham, B. VanEck, J. L. Dye, and P. B. Smith, *J. Phys. Chem.* **88,** 3852 (1984).
13. S. B. Dawes, Ph.D. Dissertation, Michigan State University, East Lansing, 1986.
14. M. J. Wagner, R. H. Huang, and J. L. Dye, *J. Phys. Chem.* **97,** 3982 (1993).
15. D. Issa, A. Ellaboudy, R. Janakiraman, and J. L. Dye, *J. Phys. Chem.* **88,** 3847 (1984).
16. D. L. Ward, R. H. Huang, M. E. Kuchenmeister, and J. L. Dye, *Acta Crystallogr. Sect. C* **46,** 1831 (1990).
17. S. B. Dawes, J. L. Eglin, K. J. Moeggenborg, J. Kim, and J. L. Dye, *J. Am. Chem. Soc.* **113,** 1605 (1991).
18. D. J. Singh, H. Krakauer, C. Haas, and W. E. Pickett, *Nature* **365,** 39 (1993).
19. J. L. Dye, *Nature* **365,** 10 (1993).
20. J. L. Dye, *Science* **247,** 663 (1990).
21. R. H. Huang, M. K. Faber, K. J. Moeggenborg, D. L. Ward, and J. L. Dye, *Nature* **331,** 599 (1988).
22. M. J. Wagner, R. H. Huang, J. L. Eglin, and J. L. Dye, *Nature* **368,** 726 (1994).
23. J. Kim, Ph.D. Dissertation, Michigan State University, East Lansing, 1989.
24. J. L. Dye, *J. Phys. Chem.* **88,** 3842 (1984).
25. J. L. Dye, M. J. Wagner, G. Overney, T. F. Nagy, and, D. Tománek, to appear.
26. Advanced Visual Systems, Inc., 300 Fifth Ave., Waltham, MA 02154.
27. R. Orbach, *Phys. Rev.* **115,** 1181 (1959).
28. W. E. Hatfield and L. W. ter Haar, *Annu. Rev. Mater. Sci.* **12,** 177 (1982).

29. L. N. Bulaevskii, A. V. Zvarykina, Y. S. Karimov, B. B. Lyubovskii, and I. F. Shchegolev, *Sov. Phys. JETP Engl. Trans.* **35,** 384 (1972).
30. Z. G. Soos and S. R. Bondeson, *Mol. Cryst. Liq. Cryst.* **85,** 19 (1982).
31. W. D. Knight, *Phys. Rev.* **76,** 1259 (1944).
32. N. F. Ramsey, *Phys. Rev.* **86,** 243 (1952).
33. P. Sheng, B. Abeles, and Y. Arie, *Phys. Rev. Lett.* **31,** 44 (1973).
34. C. J. Adkins, *J. Phys. C* **20,** 235 (1987).
35. Q. Li, L. Cruz, and P. Phillips, *Phys. Rev. B* **47,** 1840 (1993).
36. A. L. Efros and B. I. Shklovskii, *J. Phys. C* **8,** 149 (1975).
37. N. F. Mott and M. Daveh, *Adv. Phys.* **34,** 329 (1985).
38. J. E. Hendrickson, M. J. Wagner, and J. L. Dye, to appear.